



SCUOLA INTERNAZIONALE SUPERIORE DI STUDI AVANZATI

SISSA Digital Library

Many-body breakdown of indirect gap in topological Kondo insulators

Original

Many-body breakdown of indirect gap in topological Kondo insulators / Wysockiński, Marcin Mateusz; Fabrizio, Michele. - In: PHYSICAL REVIEW. B. - ISSN 2469-9950. - 94:12(2016), pp. 1-5.
[10.1103/PhysRevB.94.121102]

Availability:

This version is available at: 20.500.11767/48586 since: 2023-08-08T10:32:32Z

Publisher:

Published

DOI:10.1103/PhysRevB.94.121102

Terms of use:

Testo definito dall'ateneo relativo alle clausole di concessione d'uso

Publisher copyright

APS - American Physical Society

This version is available for education and non-commercial purposes.

note finali coverpage

(Article begins on next page)

Many-body breakdown of indirect gap in topological Kondo insulators

Marcin M. Wysocki^{1,2,*} and Michele Fabrizio^{1,†}

¹*International School for Advanced Studies (SISSA), via Bonomea 265, IT-34136, Trieste, Italy*

²*Marian Smoluchowski Institute of Physics, Jagiellonian University,
ulica prof. S. Lojasiewicza 11, PL-30-348 Kraków, Poland*

(Dated: October 2, 2018)

We show that the inclusion of nonlocal correlation effects in a variational wave function for the ground state of a topological Anderson lattice Hamiltonian is capable of describing both topologically trivial insulating phases and nontrivial ones characterized by an indirect gap, as well as its closure at the transition into a metallic phase. The method, though applied to an oversimplified model, thus captures the metallic and insulating states that are indeed observed in a variety of Kondo semiconductors, while accounting for topologically nontrivial band structures.

PACS numbers: 71.27.+a, 71.30.+h, 03.65.Vf

Introduction. Phenomena at the crossroads of topological insulators and strongly correlated systems have recently gained a lot of attention, mainly stimulated by theoretical proposals that the inclusion of strong correlations in specific models with a nontrivial topological content may give rise to novel and interesting phenomena [1–5]. However, electronic correlations in most of the discovered topological insulators [6, 7] seem to be relatively weak, and hence of minor importance. For that reason, the concept of topological Kondo insulators (TKIs) originally put forward in Refs. [8] and [9] is particularly appealing due to its possible realization in already known Kondo insulating compounds [10]. Notably, SmB_6 is convincingly confirmed to be a TKI [11–19] with strong evidence of the essential role played by many-body correlations [20, 21].

Theoretically, the main physical properties of TKI are frequently described in the framework of topological Anderson lattice models in which strong spin-orbit coupling is encoded into a spin-dependent hybridization with odd parity in momentum space [8, 9, 22]. Many-body correlations in these models have been mostly treated by the slave-boson approach or by the dynamical mean-field theory (DMFT), and predicted to induce quantum phase transitions between topologically distinct bulk insulating phases [22–24].

The aim of this work is to demonstrate that accounting for nonlocal spatial correlations, beyond those already well captured by the mentioned techniques, plays an important role in modeling TKIs. Specifically, those nonlocal correlations supply the f electron self-energy with a momentum dependence, which is otherwise purely local within DMFT and at the saddle point of the slave-boson theory. Remarkably, such a momentum dependence allows one to describe, above a critical interaction strength, the emergence of a topological Kondo insulator with an indirect gap, and its subsequent closure at the transition into a metallic state, an intriguing result *opposite* to the conventional Mott phenomenon where increasing interaction instead favours the onset of an insulating state. We disclose this scenario in two dimensions by means of the

diagrammatic expansion of the Gutzwiller wave function (GWF) technique [25, 26].

The emergence of an indirect gap [27] or its closure [28] from a model of nondispersive f orbitals, in accordance with their large mutual distance in actual materials [29, 30], is relevant to candidate TKIs, e.g., SmB_6 , but also to other $4f$ compounds not yet excluded to host topologically nontrivial states, which show bulk insulating behavior ($\text{Ce}_3\text{Bi}_4\text{Pt}_3$ [31], YbB_{12} [32], CeRhAs [33]) as well as metallic one (CeNiSn [28], CeRhSb [34], CeIrSb [35]). Moreover, assuming that increasing pressure roughly corresponds to reducing the interaction strength, we can qualitatively account for the nonuniversal behavior of the gap as observed in several Kondo semiconductors [33, 36–40].

Model and method. Our starting point is the topological Anderson lattice model on a square lattice,

$$\mathcal{H} = \sum_{\mathbf{i}, \mathbf{j}} t_{\mathbf{ij}} \hat{c}_{\mathbf{i}}^\dagger \hat{c}_{\mathbf{j}} - \sum_{\mathbf{i}} \left(\mu \hat{c}_{\mathbf{i}}^\dagger \hat{c}_{\mathbf{i}} + (\mu - \varepsilon_f) \hat{f}_{\mathbf{i}}^\dagger \hat{f}_{\mathbf{i}} + U n_{\mathbf{i}\uparrow}^f n_{\mathbf{i}\downarrow}^f \right) + \sum_{\langle \mathbf{i}, \mathbf{j} \rangle_{\alpha}, \alpha=x,y} \left(iV \left(\hat{c}_{\mathbf{i}}^\dagger \sigma_{\alpha} \hat{f}_{\mathbf{j}} + \hat{f}_{\mathbf{i}}^\dagger \sigma_{\alpha} \hat{c}_{\mathbf{j}} \right) + \text{H.c.} \right), \quad (1)$$

where the two-component spinors $\hat{f}_{\mathbf{i}}^\dagger \equiv (f_{\mathbf{i}\uparrow}^\dagger, f_{\mathbf{i}\downarrow}^\dagger)$, and accordingly for $\hat{c}_{\mathbf{i}}^\dagger$, describe localised (f) and conduction (c) electrons, $\sigma_{(\alpha=x,y)}$ are the Pauli matrices, and $\langle \mathbf{i}, \mathbf{j} \rangle_{\alpha}$ denote pairs of nearest-neighbor sites in the $\alpha = x, y$ direction. The nontrivial topology resulting from spin-orbit coupling is encoded in the odd-parity hybridization between f and c electrons [8, 9, 22]. Throughout this work we shall assume nearest neighbor c - c hopping $t = -1$, and c - f hybridization $V = 0.5$.

We study the model Eq. (1) with a variational GWF $|\psi_G\rangle \equiv \mathcal{P}_G |\psi_0\rangle \equiv \prod_{\mathbf{i}} \mathcal{P}_{\mathbf{i}} |\psi_0\rangle$ constructed from a Slater determinant, $|\psi_0\rangle$ modified by the application of local linear operators $\mathcal{P}_{\mathbf{i}}$ defined through [41]

$$\mathcal{P}_{\mathbf{i}}^\dagger \mathcal{P}_{\mathbf{i}} = \mathcal{P}_{\mathbf{i}}^2 \equiv \mathbf{1} + x d_{\mathbf{i}}, \quad (2)$$

where x is a variational parameter,

$$d_i = \left(n_{i\uparrow}^f - \langle n_{i\uparrow}^f \rangle_0 \right) \left(n_{i\downarrow}^f - \langle n_{i\downarrow}^f \rangle_0 \right), \quad (3)$$

and hereafter $\langle \dots \rangle_0$ and $\langle \dots \rangle_G$ shall denote the normalised averages over the Slater determinant, $|\psi_0\rangle$, and the GWF, $|\psi_G\rangle$, respectively. Eq. (2) allows one to write the exact expectation value of any operator \mathcal{O}_I that involves sites $I = \{\mathbf{i}_1, \mathbf{i}_2, \dots, \mathbf{i}_M\}$ as a power series in the parameter x ,

$$\begin{aligned} \langle \mathcal{O}_I \rangle_G &= \frac{1}{\langle \psi_G | \psi_G \rangle} \left\langle \mathcal{O}_I^G \prod_{\mathbf{i} \notin I} \mathcal{P}_i^2 \right\rangle_0 \\ &= \frac{1}{\langle \psi_G | \psi_G \rangle} \sum_{k=0}^{\infty} \frac{x^k}{k!} \sum'_{\mathbf{i}_1, \dots, \mathbf{i}_k} \left\langle \mathcal{O}_I^G d_{\mathbf{i}_1} d_{\mathbf{i}_2} \dots d_{\mathbf{i}_k} \right\rangle_0, \end{aligned} \quad (4)$$

where $\mathcal{O}_I^G \equiv \prod_{\mathbf{i} \in I} \mathcal{P}_i^\dagger \mathcal{O}_I \prod_{\mathbf{j} \in I} \mathcal{P}_j$. The primed summation is restricted to sites $\notin I$. The expectation values in Eq. (4) are evaluated by means of the Wick's theorem.

The popular Gutzwiller approximation corresponds to keep just the $k = 0$ term in Eq. (4) [26], which is in fact the only term that survives in the limit of infinite dimensions. In this simple case the variational optimization reduces to fix a single parameter, namely, the double occupancy of f electrons. To account for nonlocal spatial correlations in finite dimensions, higher orders of the expansion ($k > 0$) are systematically incorporated in Eq. (4) and expectation values of the products of the operators are evaluated diagrammatically [25, 26, 42–47]. By construction [25], the convergence of the sum with respect to k is reached relatively quickly, and here we found that $k = 4$ is already satisfying (see the Supplemental Material [48]). We emphasize that the convergence is not related to x being a small expansion parameter, but rather to the fast decrease of the expectation values at subsequent orders. For numerical tractability, we must set a real-space cut-off distance beyond which we neglect in Eq. (4) the contribution of the nonlocal components of the single-particle density matrix $C_{\mathbf{r}, \mathbf{0}}^{\alpha, \beta} \equiv \langle \alpha_{\mathbf{r}\sigma}^\dagger \beta_{\mathbf{0}\sigma'} \rangle_0$, where $\alpha, \beta \in \{f, c\}$, $\sigma = \sigma'$ for C^{ff} and C^{cc} , and $\sigma = -\sigma'$ for C^{cf} . Specifically we choose $|\mathbf{r}|^2 \leq 5$ for C^{ff} and $|\mathbf{r}|^2 \leq 2$ for C^{cf} (in units of the lattice constant).

It is known that a faithful variational description of correlated systems in finite dimensions requires going beyond the simple GWF by adding longer-range correlations via Jastrow-like operators [49, 50], whose optimization can, however, be accomplished only by variational Monte Carlo techniques. Alternatively, one could be satisfied with just the GWF result Eq. (4) at higher orders in $k > 0$ on the provision that the uncorrelated Slater determinant is also modified accordingly so as to minimize the total energy. This approach, though less accurate, is numerically less demanding and provides results already in the thermodynamic limit. Despite the simple form of the variational GWF, this method frequently yields

results in accordance with the variational Monte Carlo [42, 43].

The expectation value of the Hamiltonian (1), $\langle \mathcal{H} \rangle_G$ is evaluated diagrammatically according to Eq. (4), and subsequently optimized with respect to the variational parameter x and to the single-particle Hamiltonian whose ground state is $|\psi_0\rangle$ (for details, see the Supplemental Material [48]), which turns out to have the general expression

$$\begin{aligned} \mathcal{H}^{\text{eff}} &= \sum_{\mathbf{i}, \mathbf{j}} t_{\mathbf{i}\mathbf{j}} \hat{c}_i^\dagger \hat{c}_j + \sum_{\mathbf{i}, \mathbf{j}} t_{\mathbf{i}\mathbf{j}}^f \hat{f}_i^\dagger \hat{f}_j \\ &+ \sum_{\langle \mathbf{i}, \mathbf{j} \rangle, \alpha=x, y} \left[iV_{\mathbf{i}\mathbf{j}}^{\text{eff}} \left(\hat{c}_i^\dagger \sigma_\alpha \hat{f}_j + \hat{f}_i^\dagger \sigma_\alpha \hat{c}_j \right) + \text{H.c.} \right] \\ &+ \sum_{\langle \langle \mathbf{i}, \mathbf{j} \rangle \rangle} \left\{ iV_{\mathbf{i}\mathbf{j}}^{\text{eff}} \left[\hat{c}_i^\dagger (\sigma_x - a\sigma_y) \hat{f}_j + \hat{f}_i^\dagger (\sigma_x - a\sigma_y) \hat{c}_j \right] + \text{H.c.} \right\} \\ &\equiv \sum_{\mathbf{k}} \hat{\Psi}_{\mathbf{k}}^\dagger \hat{\mathcal{H}}^{\text{eff}}(\mathbf{k}) \hat{\Psi}_{\mathbf{k}}, \end{aligned} \quad (5)$$

where $\hat{\Psi}_{\mathbf{k}} = (\hat{c}_{\mathbf{k}}, \hat{f}_{\mathbf{k}})$ are four-component spinors in momentum space, $t_{\mathbf{i}\mathbf{i}}$ and $t_{\mathbf{i}\mathbf{i}}^f$ are the on-site energies of the c and f electrons, respectively, $\langle \langle \mathbf{i}, \mathbf{j} \rangle \rangle$ denotes the sum over next-to-nearest neighbors, and by convention, $a = \pm 1$ for bonds in the $(1, \pm 1)$ direction.

In other words, the optimization of inter-site correlations in Eq. (4) leads to an effective single-particle Hamiltonian (5) that includes further neighbors c - f hybridization as well as a direct long-range f - f hopping. On the contrary, since \mathcal{P}_G does not act on the c electrons, the nearest-neighbor c - c hopping amplitude is that of the original Hamiltonian.

The topological properties of the model may be inferred already from the effective Hamiltonian $\hat{\mathcal{H}}^{\text{eff}}(\mathbf{k}^*)$, Eq. (5), which at the time reversal invariant momenta, \mathbf{k}^* , can be casted into the form [8],

$$2\hat{\mathcal{H}}^{\text{eff}}(\mathbf{k}^*) = \left[\epsilon_c(\mathbf{k}^*) + \epsilon_f(\mathbf{k}^*) \right] \mathbb{I} + \left[\epsilon_c(\mathbf{k}^*) - \epsilon_f(\mathbf{k}^*) \right] \mathbb{P},$$

where \mathbb{I} is the identity and \mathbb{P} the diagonal parity operator with elements $+1$ for c and -1 for f , while the c and f dispersions, $\epsilon_c(\mathbf{k})$ and $\epsilon_f(\mathbf{k})$, are derived from Eq. (5). The Z_2 topological invariant ν [51] can be readily obtained [52] from $(-1)^\nu = \prod_i \delta_i$ with $\delta_i = \text{sgn}[\epsilon_c(\mathbf{k}_i^*) - \epsilon_f(\mathbf{k}_i^*)]$, where the product runs over the four \mathbf{k}^* -points: Γ , X, Y and M. By symmetry X and Y are equivalent.

Results. We mentioned that the model, Eq. (1), with nondispersive f states should hopefully describe putative TKIs such as SmB₆ with indirect gaps between the valence and conduction bands [27, 53]. However, the mean-field treatment of the Hamiltonian (1) at half filling leads instead to a semimetal because of the vanishing hybridization at \mathbf{k}^* . By contrast, mean-field theory applied to models for Kondo insulators with even-parity hybridization does lead to the desired insulating state. To

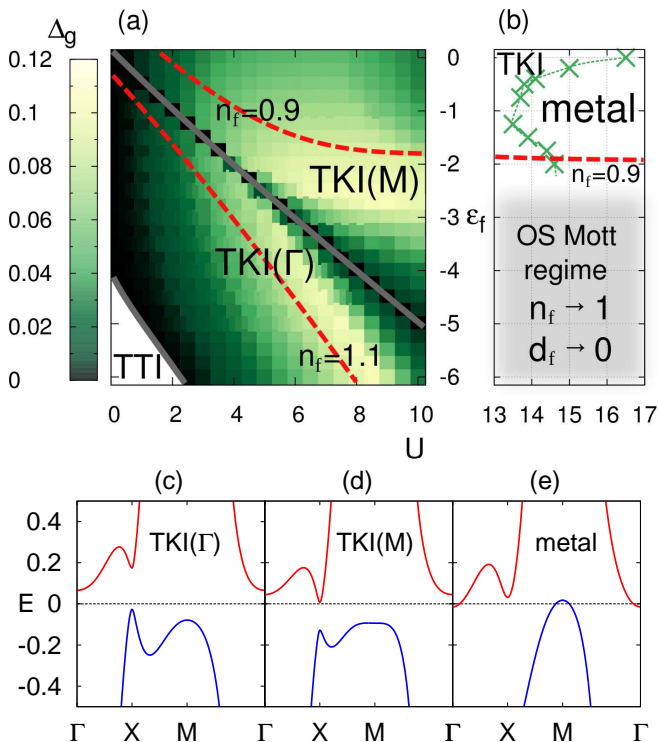


FIG. 1: (a) U vs. ε_f phase diagram of the model (1) at half-filling, with the value of the emergent indirect gap marked on a color scale. The phase diagram comprises three topologically distinct phases, a trivial topological insulator (TTI) and two nontrivial ones, TKI(Γ) and TKI(M). Along the two red dashed lines the f occupancy is constant, with $n_f = 0.9$ and $n_f = 1.1$. (b) The continuation of the phase diagram for larger U where the TKI can undergo a transition to a metallic state. The region where the f occupancy locks at $n_f = 1$ with negligible fluctuations, $d_f \rightarrow 0$, is denoted as an orbital selective (OS) Mott regime. (c-e) Exemplary low energy band structures for the selected phases: (c) TKI(Γ) for $U = 7$ and $\varepsilon_f = -5$; (d) TKI(M) for $U = 9$ and $\varepsilon_f = -2.5$; (e) metal for $U = 20$ and $\varepsilon_f = -0.5$. The valence and the conduction bands are marked with different colors.

cure the inadequacy of mean-field and recover an insulator with an indirect gap, *ad hoc* dispersion of f electrons is frequently assumed [23, 24], whose minimum in the Brillouin zone is shifted by (π, π) from that of conduction electrons. However, such an additional ingredient is not truly justified, e.g., in SmB_6 , where the large separation between $4f$ elements [29], hence their negligible mutual overlap, implies that the main source of f itinerancy remains the c - f hybridization. We mention that spin-polarized local density approximation (LSDA)+ U calculations [54] suggest a sizable f - f hopping mediated by the hybridization with boron p states. We suspect this is rather an artifact of the method that artificially pushes spin-majority f states down to the occupied boron p bands. In reality, such boron mediated hopping should be fairly negligible at the Fermi level.

In our present attempt to go beyond the mean field, a direct f - f hopping amplitude t^f is variationally gener-

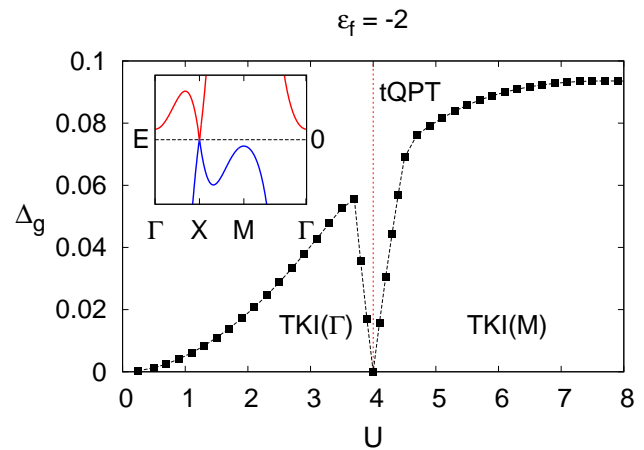


FIG. 2: Evolution of the indirect gap Δ_g with increasing U across the topological quantum phase transition (tQPT) between TKI(Γ) and TKI(M) at $\varepsilon_f = -2$. The inset shows the low energy band structure at the topological phase transition where both direct and indirect gaps close, which indicates that the TKI(Γ) and TKI(M) are phases not adiabatically connected.

ated, hence we do not need to include it to get sensible physical results. In particular, for moderate values of U , the generated nearest neighbor f - f hopping has an opposite sign to its c - c counterpart t , which is convenient to open an indirect gap. In fact, the best situation to open a hybridization gap between two overlapping bands occurs when they cross with opposite slopes, which is exactly what our variational wave function does to minimize the energy. The value of the indirect gap Δ_g that we find is shown as a color plot in the phase diagram of Fig. 1(a).

In terms of the topologically distinct phases in the present lattice geometry [23, 55], we find [see Fig. 1(a)] topologically trivial insulators (TTIs) as well as topologically nontrivial Kondo insulating phases: TKI(Γ) with the parities $\delta_i = (-1, 1, 1, 1)$ and TKI(M) with $\delta_i = (-1, 1, -1, -1)$, where $i \in \{\Gamma, M, X, Y\}$. The exemplary low energy band structures for TKI(Γ) and TKI(M) are drawn in Figs. 1(c) and 1(d). The topological phase transition between these two phases significantly influences the behavior of the indirect gap.

The largest values of the gap are attained above $U \sim 4$ and are roughly enclosed within the f isovalent regions with $n_f \simeq 0.9$ and $n_f \simeq 1.1$ [cf. Fig.1(a)], where n_f is the average f electron number per lattice site. The intuitive expectation that the effect of correlations is more pronounced the closer the f orbital is at the half-filling thus fails in the vicinity of the TKI(Γ)-TKI(M) transition for $n_f \simeq 1$, marked with a solid gray line in Fig. 1(a). This topological phase transition enforces the closure of the band gap (both direct and indirect) [23] and leads to its rapid decrease in its neighborhood (see Fig. 2). We note that, even though the behavior of the gap versus U

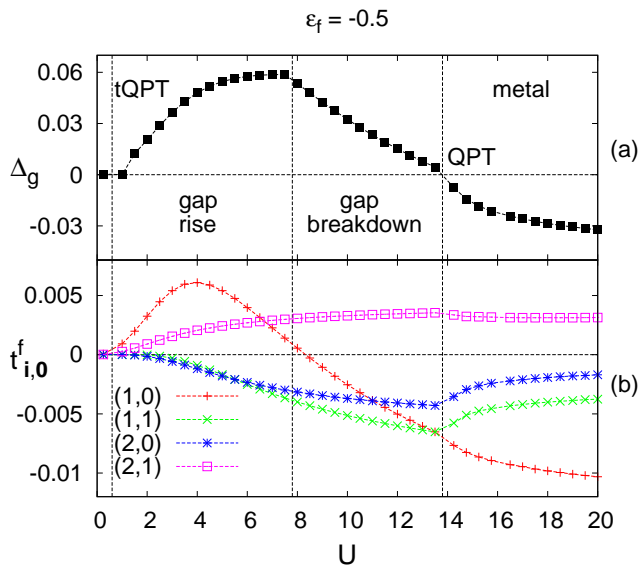


FIG. 3: Evolution vs U of (a) the indirect gap Δ_g ; (b) the variationally generated f - f hopping amplitudes t^f . Three regimes are identified: (i) initial rise of the gap; (ii) its collapse associated with the sign change of the nearest neighbor [$\mathbf{r} = (1,0)$] t^f ; (iii) the metallic state characterized by the negative value of Δ_g , namely by overlapping valence and conduction bands, after a quantum phase transition (QPT). We also mark the topological quantum phase transition (tQPT) for small $U \simeq 0.5$.

at $\varepsilon = -2$ (Fig. 2) is different from the DMFT results of Ref. [23], not surprisingly since we do not include any finite f - f hopping, nevertheless the value $U \simeq 4$ for the topological transition is coincident.

In Fig. 1(b), we show the phase diagram at larger values of the Coulomb repulsion. Here and for $\varepsilon_f \gtrsim -2$, upon increasing U , the system undergoes a transition from a TKI to a metal [see Fig.1(e) for an exemplary low energy band structure]. On the contrary, for $\varepsilon_f \lesssim -2$, we find an orbital-selective Mott state where the f occupancy is pinned to $n_f = 1$ with vanishingly small fluctuations, $d_f \rightarrow 0$.

In Fig. 3(a) we plot the evolution of Δ_g with increasing U for $\varepsilon_f = -0.5$. In this plot we have singled out three stages: (i) the initial rise of the gap, (ii) its subsequent drop till (iii) its sign change, which signals that the two bands now overlap, yielding a metallic behavior. We also mark the topological transition between TKI(Γ) and TKI(M) at small $U \simeq 0.5$. It seems that the crucial factor leading to the nonmonotonic gap behavior is just the effective f - f hopping that is variationally generated. In Fig. 3(b), we show the U dependence of the f - f hopping amplitudes, $t^f_{i,0}$, with different $\mathbf{i} = (n, m)$. We observe that the downturn of Δ_g occurs close to the value of U at which the nearest-neighbor hopping, i.e., $\mathbf{i} = (1,0)$, changes sign, from being opposite to the c - c

hopping to being concordant. However, the sign change is still not enough to close the gap, since in the meantime sizable further-neighbor hopping has been generated: second, $\mathbf{i} = (1,1)$, third, $\mathbf{i} = (2,0)$, and fourth neighbor, $\mathbf{i} = (2,1)$, ones. Eventually, when the negative nearest-neighbor hopping overwhelms the others, the gap closes.

We can attempt to rationalize the observed nontrivial behavior of the direct f - f hopping by simple arguments. Given that the Hamiltonian, Eq. (1), lacks such hopping process, the expectation value $\langle f_i^\dagger f_j \rangle$ between nearest-neighbor sites on the true ground state is finite only because of c - f hybridization and has an opposite sign to $\langle c_i^\dagger c_j \rangle$ for any U . Since the latter hampers the f electron motion, it must reduce the value of $|\langle f_i^\dagger f_j \rangle|$ with respect to the noninteracting $U = 0$ case. In a variational approach such as ours, based on a wave function obtained as the ground state of an auxiliary noninteracting Hamiltonian \mathcal{H}^{eff} modified by the action of local operators \mathcal{P}_i , this reduction can be attained in two ways: by lowering the c - f hybridization V^{eff} in \mathcal{H}^{eff} and/or by generating a nearest-neighbor f - f hopping t^f of the same sign as the c - c one, i.e., negative in our case. When U is large, the optimized Hamiltonian \mathcal{H}^{eff} indeed comprises a finite $t^f < 0$, which, in addition to the lowering of V^{eff} , allows one to reduce $|\langle f_i^\dagger f_j \rangle|$. This result agrees with more accurate variational approaches in the large- U limit of the Kondo lattice model [56]. On the contrary, for small to intermediate values of U , the system prefers to generate a positive $t^f > 0$, which, as we mentioned, favors the opening of a hybridization gap.

Summary. The results we have obtained might be relevant to known Kondo semiconductors [10] and are promising in view of possible topologically nontrivial states. The wealth of phases that we find, ranging from nontopological to topological insulators and metals, are indeed observed in different compounds [27, 28, 31, 32, 34, 35]. Moreover, the nonmonotonic behavior of the indirect gap with respect to the strength of U brings to mind the variety of responses observed under pressure in Kondo semiconductors, ranging from a gap decrease in SmB_6 [39, 40] and in CeRhAs [33], to its increase in $\text{Ce}_3\text{Bi}_4\text{Pt}_3$ [37] and in CeNiSn [36], and finally to the nonmonotonic evolution as seen in CeRhSb [38]. We also note that the semimetal phase, which appears once the indirect gap closes and still possesses topologically nontrivial properties, mimics exactly the physical scenario proposed for CeNiSn [8, 57] to explain its intriguing properties [57–60]. The precise sequence and topological properties of the phases that we find must evidently depend on our choice of model and lattice geometry. However, it is encouraging that the same method gives access to all those phases, including topologically nontrivial ones, especially in view of applications to more realistic modeling.

In summary we have shown that the Anderson lattice model Eq. (1) can support a topological insulating state stabilized purely by correlations. In particular, we found variationally that the impurity self-energy acquires the right momentum dependence to open a gap, despite the fact that, from the start, the model does not include any direct hopping between the f orbitals. It is now worth comparing our results with recent ones on SmB_6 based on a combined LDA plus Gutzwiller technique [20]. Within LDA the spin-orbit split f orbitals give rise to narrow bands of width $W \sim 0.5$ eV around the Fermi level with a semiconducting behavior characterized by a direct gap $\Delta \sim 15$ meV. The inclusion of local Gutzwiller correlations brings about a sizable reduction of quasiparticle weight, $z \sim 0.18$, which reduces the $j = 5/2$ bandwidth to $W_* \sim zW \sim 0.1$ eV, the $j = 7/2$ f bands being pushed up to 4.0 eV above the Fermi level [20]. Despite such a small value of z , the semiconducting behavior survives local correlations. The direct gap is almost unchanged, although a smaller indirect gap of ~ 10 meV emerges. Although this result is well in accordance with ours, the mechanism that stabilises the gap might at first glance appear to be different, since in the case of Ref. [20] the LDA band structure is already semiconducting, which, as we mentioned, implies a finite f - f hopping. However, since LDA already includes some correlation effects, it is not clear whether the f - f hopping is a one- or many-body effect. The fact that the gap is almost unaffected by the reduction of quasiparticle weight that would renormalize down any one-body hopping term, might suggest that the LDA f dispersion already includes nonlocal correlation effects, thus in agreement with our calculations. Further investigations would be desirable to assess this issue.

Acknowledgements. MMW is grateful for discussions with A. Amaricci, and greatly acknowledges the support from Polish Ministry of Science and Higher Education under the ‘‘Mobilność Plus’’ program, Agreement No. 1265/MOB/IV/2015/0.

* Electronic address: mwysoki@sissa.it

† Electronic address: fabrizio@sissa.it

- [1] M. Hohenadler and F. F. Assaad, *Journal of Physics: Condensed Matter* **25**, 143201 (2013).
- [2] S. Raghu, X.-L. Qi, C. Honerkamp, and S.-C. Zhang, *Phys. Rev. Lett.* **100**, 156401 (2008).
- [3] K. Sun, H. Yao, E. Fradkin, and S. A. Kivelson, *Phys. Rev. Lett.* **103**, 046811 (2009).
- [4] K. Sun, W. V. Liu, A. Hemmerich, and S. Das Sarma, *Nat. Phys.* **8**, 67 (2012).
- [5] A. Amaricci, J. C. Budich, M. Capone, B. Trauzettel, and G. Sangiovanni, *Phys. Rev. Lett.* **114**, 185701 (2015).
- [6] M. Z. Hasan and C. L. Kane, *Rev. Mod. Phys.* **82**, 3045 (2010).
- [7] X.-L. Qi and S.-C. Zhang, *Rev. Mod. Phys.* **83**, 1057 (2011).
- [8] M. Dzero, K. Sun, V. Galitski, and P. Coleman, *Phys. Rev. Lett.* **104**, 106408 (2010).
- [9] M. Dzero, K. Sun, P. Coleman, and V. Galitski, *Phys. Rev. B* **85**, 045130 (2012).
- [10] P. S. Riseborough, *Advances in Physics* **49**, 257 (2000).
- [11] M. Neupane, N. Alidoust, S.-Y. Xu, T. Kondo, Y. Ishida, D. J. Kim, C. Liu, I. Belopolski, Y. J. Jo, T.-R. Chang, et al., *Nat. Commun.* **4**, 2991 (2013).
- [12] J. Jiang, S. Li, T. Zhang, Z. Sun, F. Chen, Z. Ye, M. Xu, Q. Ge, S. Tan, X. Niu, et al., *Nat. Commun.* **4**, 3010 (2013).
- [13] S. Wolgast, C. Kurdak, K. Sun, J. W. Allen, D.-J. Kim, and Z. Fisk, *Phys. Rev. B* **88**, 180405 (2013).
- [14] W. Ruan, C. Ye, M. Guo, F. Chen, X. Chen, G.-M. Zhang, and Y. Wang, *Phys. Rev. Lett.* **112**, 136401 (2014).
- [15] D.-J. Kim, S. Thomas, T. Grant, J. Botimer, Z. Fisk, and J. Xia, *Sci. Rep.* **3**, 3150 (2013).
- [16] D. J. Kim, J. Xia, and Z. Fisk, *Nat. Mater.* **13**, 466 (2014).
- [17] P. Syers, D. Kim, M. S. Fuhrer, and J. Paglione, *Phys. Rev. Lett.* **114**, 096601 (2015).
- [18] Y. Luo, H. Chen, J. Dai, Z.-a. Xu, and J. D. Thompson, *Phys. Rev. B* **91**, 075130 (2015).
- [19] N. Wakeham, Y. Q. Wang, Z. Fisk, F. Ronning, and J. D. Thompson, *Phys. Rev. B* **91**, 085107 (2015).
- [20] F. Lu, J. Zhao, H. Weng, Z. Fang, and X. Dai, *Phys. Rev. Lett.* **110**, 096401 (2013).
- [21] W. T. Fuhrman, J. Leiner, P. Nikolić, G. E. Granroth, M. B. Stone, M. D. Lumsden, L. DeBeer-Schmitt, P. A. Alekseev, J.-M. Mignot, S. M. Koohpayeh, et al., *Phys. Rev. Lett.* **114**, 036401 (2015).
- [22] M.-T. Tran, T. Takimoto, and K.-S. Kim, *Phys. Rev. B* **85**, 125128 (2012).
- [23] J. Werner and F. F. Assaad, *Phys. Rev. B* **88**, 035113 (2013).
- [24] M. Legner, A. Rüegg, and M. Sigrist, *Phys. Rev. B* **89**, 085110 (2014).
- [25] J. Bünemann, T. Schickling, and F. Gebhard, *Eur. Phys. Lett.* **98**, 27006 (2012).
- [26] M. M. Wysokiński, J. Kaczmarczyk, and J. Spałek, *Phys. Rev. B* **92**, 125135 (2015).
- [27] A. Menth, E. Buehler, and T. H. Geballe, *Phys. Rev. Lett.* **22**, 295 (1969).
- [28] T. Takabatake, F. Teshima, H. Fujii, S. Nishigori, T. Suzuki, T. Fujita, Y. Yamaguchi, J. Sakurai, and D. Jaccard, *Phys. Rev. B* **41**, 9607 (1990).
- [29] N. P. Butch, J. Paglione, P. Chow, Y. Xiao, C. A. Marianetti, C. H. Booth, and J. R. Jeffries, *Phys. Rev. Lett.* **116**, 156401 (2016).
- [30] A. Hiess, I. Zokkalo, M. Bonnet, J. Schweizer, E. Lelivre-Berna, F. Tasset, Y. Isikawa, and G. H. Lander, *J. Phys.: Condens. Matter* **9**, 9321 (1997).
- [31] M. F. Hundley, P. C. Canfield, J. D. Thompson, Z. Fisk, and J. M. Lawrence, *Phys. Rev. B* **42**, 6842 (1990).
- [32] H. Okamura, S. Kimura, H. Shinozaki, T. Nanba, F. Iga, N. Shimizu, and T. Takabatake, *Phys. Rev. B* **58**, R7496 (1998).
- [33] S. Yoshii, M. Kasaya, T. Takahashi, and N. Mori, *Physica B* **223-224**, 421 (1996).
- [34] S. K. Malik and D. T. Adroja, *Phys. Rev. B* **43**, 6277 (1991).
- [35] Y. Kawasaki, M. Izumi, Y. Kishimoto, T. Ohno, H. Tou, Y. Inaoka, M. Sera, K. Shigetoh, and T. Takabatake, *Phys. Rev. B* **75**, 094410 (2007).

- [36] T. Hiraoka, E. Kinoshita, T. Takabatake, H. Tanaka, and H. Fujii, *Physica B* **199-200**, 4440 (1994).
- [37] J. C. Cooley, M. C. Aronson, and P. C. Canfield, *Phys. Rev. B* **55**, 7533 (1997).
- [38] Y. Uwatoko, T. Ishii, G. Oomi, H. Takahashi, N. Mri, J. Thompson, J. Shero, D. Madru, and Z. Fisk, *Journal of the Physical Society of Japan* **65**, 27 (1996).
- [39] S. Gabáni, E. Bauer, S. Berger, K. Flachbart, Y. Paderno, C. Paul, V. Pavlík, and N. Shitsevalova, *Phys. Rev. B* **67**, 172406 (2003).
- [40] Y. Zhou, Q. Wu, P. F. S. Rosa, R. Yu, J. Guo, W. Yi, S. Zhang, Z. Wang, W. Honghong, K. Cai, Shu Yang, et al. (2016), arXiv:1603.05607.
- [41] F. Gebhard, *Phys. Rev. B* **41**, 9452 (1990).
- [42] J. Kaczmarczyk, J. Spalek, T. Schickling, and J. Bünemann, *Phys. Rev. B* **88**, 115127 (2013).
- [43] J. Kaczmarczyk, J. Bünemann, and J. Spalek, *New J. Phys.* **16**, 073018 (2014).
- [44] A. Tomski and J. Kaczmarczyk, *Journal of Physics: Condensed Matter* **28**, 175701 (2016).
- [45] J. Kaczmarczyk, *Phil. Mag.* **95**, 563 (2015).
- [46] J. Kaczmarczyk, T. Schickling, and J. Bünemann, *Phys. Status Solidi b* **252**, 2059 (2015).
- [47] M. M. Wysokiński, J. Kaczmarczyk, and J. Spalek, *Phys. Rev. B* **94**, 024517 (2016).
- [48] See Supplemental Material at [URL] for the details of the method and the discussion of the convergence with respect to the order of diagrammatic expansion.
- [49] M. Capello, F. Becca, M. Fabrizio, S. Sorella, and E. Tosatti, *Phys. Rev. Lett.* **94**, 026406 (2005).
- [50] J. P. F. LeBlanc, A. E. Antipov, F. Becca, I. W. Bulik, G. K.-L. Chan, C.-M. Chung, Y. Deng, M. Ferrero, T. M. Henderson, C. A. Jiménez-Hoyos, et al. (Simons Collaboration on the Many-Electron Problem), *Phys. Rev. X* **5**, 041041 (2015).
- [51] C. L. Kane and E. J. Mele, *Phys. Rev. Lett.* **95**, 146802 (2005).
- [52] L. Fu and C. L. Kane, *Phys. Rev. B* **76**, 045302 (2007).
- [53] J. Demsar, V. K. Thorsmølle, J. L. Sarrao, and A. J. Taylor, *Phys. Rev. Lett.* **96**, 037401 (2006).
- [54] V. N. Antonov, B. N. Harmon, and A. N. Yaresko, *Phys. Rev. B* **66**, 165209 (2002).
- [55] R.-J. Slager, A. Mesaros, V. Juričić, and J. Zaanen, *Nat. Phys.* **9**, 98 (2013).
- [56] M. Z. Asadzadeh, F. Becca, and M. Fabrizio, *Phys. Rev. B* **87**, 205144 (2013).
- [57] P.-Y. Chang, O. Erten, and P. Coleman (2016), arXiv:1603.03435.
- [58] M. Sera, N. Kobayashi, T. Yoshino, K. Kobayashi, T. Takabatake, G. Nakamoto, and H. Fujii, *Phys. Rev. B* **55**, 6421 (1997).
- [59] T. Terashima, C. Terakura, S. Uji, H. Aoki, Y. Echizen, and T. Takabatake, *Phys. Rev. B* **66**, 075127 (2002).
- [60] A. Ślebarski and J. Spalek, *Phil. Mag.* **89**, 1845 (2009).

**Supplemental Material to the article:
“Many-body breakdown of indirect gap in topological Kondo insulators”**

**DETAILS OF THE DIAGRAMMATIC
EXPANSION FOR THE GUTZWILLER WAVE
FUNCTION TECHNIQUE**

Formal expansion

The variational analysis of the topological Anderson lattice Hamiltonian, including the non-local effects of the onsite interaction, begins with the formulation of the exact form of the expectation value with the full Gutzwiller wave function (GWF) of any operator \mathcal{O}_I that involves sites $I = \{\mathbf{i}_1, \mathbf{i}_2, \dots, \mathbf{i}_M\}$,

$$\begin{aligned} \langle \mathcal{O}_I \rangle_G &= \frac{1}{\langle \psi_G | \psi_G \rangle} \left\langle \mathcal{O}_I^G \prod_{\mathbf{i} \notin I} \mathcal{P}_I^2 \right\rangle_0 \\ &= \frac{1}{\langle \psi_G | \psi_G \rangle} \sum_{k=0}^{\infty} \frac{x^k}{k!} \sum' \left\langle \mathcal{O}_I^G d_{\mathbf{i}_1} d_{\mathbf{i}_2} \dots d_{\mathbf{i}_k} \right\rangle_0, \end{aligned} \quad (\text{S1})$$

where $\mathcal{O}_I^G \equiv \prod_{\mathbf{i} \in I} \mathcal{P}_I^\dagger \mathcal{O}_I \prod_{\mathbf{j} \in I} \mathcal{P}_j$. The expectation values in Eq. (S1) are evaluated by means of the Wick's theorem. They can be visualized by a sum of diagrams connecting sites in the real space with lines representing single particle density matrices,

$$\begin{aligned} C_{\mathbf{l}, \mathbf{l}'}^{ff} &\equiv \langle f_{\mathbf{l}\sigma}^\dagger f_{\mathbf{l}'\sigma} \rangle_0, \\ C_{\mathbf{l}, \mathbf{l}'}^{fc} &\equiv \langle c_{\mathbf{l}\sigma}^\dagger f_{\mathbf{l}'-\sigma} \rangle_0, \\ C_{\mathbf{l}, \mathbf{l}'}^{cc} &\equiv \langle c_{\mathbf{l}\sigma}^\dagger c_{\mathbf{l}'\sigma} \rangle_0, \end{aligned} \quad (\text{S2})$$

where \mathbf{l}, \mathbf{l}' are lattice indices and σ denotes (pseudo)spin index for c (f) electrons. In order to evaluate the expectation value of the topological Anderson lattice Hamiltonian first we derive the expressions for the following projected operators,

$$\begin{aligned} \mathcal{P}_i d_i \mathcal{P}_i &= \lambda_d^2 [2n_{0f} n_i^{\text{HF}} + (1 - x d_0) d_i + n_{0f}^2 \mathcal{P}_i^2], \\ \mathcal{P}_i n_{i\sigma}^f \mathcal{P}_i &= (1 + xm) n_i^{\text{HF}} + \gamma d_i + n_{0f} \mathcal{P}_i^2, \\ \mathcal{P}_i f_{i\sigma}^{(\dagger)} \mathcal{P}_i &= \alpha f_{i\sigma}^{(\dagger)} + \beta f_{i\sigma}^{(\dagger)} n_i^{\text{HF}}, \end{aligned} \quad (\text{S3})$$

where additionally we define

$$\begin{aligned} n_{i\sigma}^{\text{HF}} &\equiv n_{i\sigma}^f - \langle n_{i\sigma}^f \rangle_0 = n_{i-\sigma}^{\text{HF}} \equiv n_i^{\text{HF}} \\ n_{0f} &\equiv \langle n_{i\sigma}^f \rangle_0 \\ \beta &\equiv \lambda_s (\lambda_d - \lambda_0), \\ \alpha &\equiv \lambda_s \lambda_0 + \beta n_{0f}, \\ \gamma &\equiv x(1 - 2n_{0f}), \\ m &\equiv n_{0f}(1 - n_{0f}), \end{aligned} \quad (\text{S4})$$

where superscript HF stands for the Hartree-Fock form of the operator. Here, the parameters $\{\lambda_0, \lambda_s, \lambda_d\}$ have

the following meaning. The general, diagonal Gutzwiller correlator acting on the f electrons can be written as,

$$\mathcal{P}_i = \sum_{\Gamma} \lambda_{\Gamma} |\Gamma\rangle_i \langle \Gamma|_i, \quad (\text{S5})$$

with variational parameters $\lambda_{\Gamma} \in \{\lambda_0, \lambda_{\uparrow}, \lambda_{\downarrow}, \lambda_d\}$ that characterize the occupation probabilities for the four possible atomic Fock f -states $|\Gamma\rangle_i \in \{|0\rangle_i, |\uparrow\rangle_i, |\downarrow\rangle_i, |\uparrow\downarrow\rangle_i\}$. By constraining the correlator with Eq. (2) (main manuscript) we obtain

$$\begin{aligned} \lambda_0^2 &= 1 + x n_{0f}^2, \\ \lambda_{\sigma}^2 &= \lambda_{-\sigma}^2 \equiv \lambda_s^2 = 1 - x n_{0f}(1 - n_{0f}), \\ \lambda_d^2 &= 1 + x(1 - n_{0f})^2. \end{aligned} \quad (\text{S6})$$

The diagrammatic sums for the operators resulting from (S3) are expressed as

$$S = \sum_{k=0}^{\infty} \frac{x^k}{k!} S(k), \quad (\text{S7})$$

where $S \in \{T_{\mathbf{i}, \mathbf{i}+\mathbf{x}}^{(1,1)}, T_{\mathbf{i}, \mathbf{i}+\mathbf{x}}^{(1,3)}, I^{(4)}, I^{(2)}\}$, and the k -th order contributions $S(k)$ read,

$$\begin{aligned} T_{\mathbf{i}, \mathbf{i}+\mathbf{x}}^{(1,1[3])}(k) &\equiv \sum_{\mathbf{l}_1, \dots, \mathbf{l}_k} \langle c_{\mathbf{l}\sigma}^\dagger [n_{\mathbf{l}\sigma}^{\text{HF}}] f_{\mathbf{i}+\mathbf{x}, -\sigma} d_{\mathbf{l}_1, \dots, \mathbf{l}_k} \rangle_0^c \\ I^{(4)}(k) &\equiv \sum_{\mathbf{l}_1, \dots, \mathbf{l}_k} \langle d_{\mathbf{l}_1} d_{\mathbf{l}_2} \dots d_{\mathbf{l}_k} \rangle_0^c, \\ I^{(2)}(k) &\equiv \sum_{\mathbf{l}_1, \dots, \mathbf{l}_k} \langle n_{\mathbf{l}_1}^{\text{HF}} d_{\mathbf{l}_2} \dots d_{\mathbf{l}_k} \rangle_0^c. \end{aligned} \quad (\text{S8})$$

Here superscript c denotes only fully connected diagrams [1], because, with the help of the linked-cluster theorem waiving the summation restriction, GWF norm cancels out all the disconnected diagrams.

In the Eqs. (S3) we have expressed the projected operators by their HF or relative forms as it significantly speeds up the convergence of the numerical results concerning the summation of the diagrams [1]. It is attributed to the fact that by such a construction, all the two-operator averages for a single site and f -orbital (so-called *Hartree bubbles*) automatically vanish.

Conservation of the number of electrons

Before the explicit evaluation of the expectation value of the topological Anderson lattice Hamiltonian with the GWF one issue, particularly important for the modelling of Kondo insulators, still needs to be resolved. Due to the

fact that the Gutzwiller correlator has a diagonal form and acts only on the f degrees of freedom it commutes not only with the operator of the total number of particles but also with those of f and c number of electrons separately. This yields following equities,

$$\begin{aligned}\langle c_{i\sigma}^\dagger c_{i\sigma} \rangle_G &= \langle c_{i\sigma}^\dagger c_{i\sigma} \rangle_0, \\ \langle f_{i\sigma}^\dagger f_{i\sigma} \rangle_G &= \langle f_{i\sigma}^\dagger f_{i\sigma} \rangle_0.\end{aligned}\quad (\text{S9})$$

It is not automatically satisfied in our approach because of the real-space and the order cut-offs introduced [2]. However, it can be straightforwardly enforced by the construction. Due to the odd hybridization, introducing symmetric cancellation of the diagrams in the real space, the averages of the pairs of c operators for all \mathbf{i} and \mathbf{j} , are the same when taken with either $|\psi_0\rangle$ or $|\psi_G\rangle$,

$$\langle c_{i\sigma}^\dagger c_{j\sigma} \rangle_G = \langle c_{i\sigma}^\dagger c_{j\sigma} \rangle_0. \quad (\text{S10})$$

Therefore, what remains, is to ensure that $\langle f_{i\sigma}^\dagger f_{i\sigma} \rangle_G = \langle f_{i\sigma}^\dagger f_{i\sigma} \rangle_0$. The *correlated* (averaged with the GWF) number of f electrons can be rewritten in the following form (cf. Eq. (S3)),

$$\langle f_{i\sigma}^\dagger f_{i\sigma} \rangle_G = n_{0f} + (1 + xm)I^{(2)} + \gamma I^{(4)}. \quad (\text{S11})$$

The conservation of the total number of particles can be now enforced by the construction by imposing the cancellation of the sum of the two last terms in Eq. (S11) [1], which reduces to the following relation

$$I^{(2)} = \frac{-\gamma}{1 + xm} I^{(4)}. \quad (\text{S12})$$

As a result we calculate diagrammatically only $I^{(4)}$, which due to its structure introduces less error connected with the real-space cut-off than $I^{(2)}$. [2]

Expectation value of the Hamiltonian and the derivation of its single-particle effective correspondent

The resulting expectation value of the topological Anderson lattice Hamiltonian with the GWF can be readily expressed as following (σ and lattice summations are already executed),

$$\frac{\langle \mathcal{H} \rangle_G}{L} = 8tC_{\mathbf{i},\mathbf{i}+\mathbf{x}}^{cc} - 2\mu C_{\mathbf{i},\mathbf{i}}^{cc} - 2(\mu - \varepsilon_f)n_{0f} + U\lambda_d^2 \left(n_{0f}^2 + \frac{\lambda_s^2 \lambda_0^2}{1 + mx} I^{(4)} \right) + 16V \left(\alpha T_{\mathbf{i},\mathbf{i}+\mathbf{x}}^{(1,1)} + \beta T_{\mathbf{i},\mathbf{i}+\mathbf{x}}^{(1,3)} \right), \quad (\text{S13})$$

where L denotes the number of the lattice sites and \mathbf{x} is a vector in the \mathbf{x} -direction with the length of the lattice constant. Calculated diagrammatically $\langle \mathcal{H} \rangle_G$ is first optimized with respect to the variational parameter x . Then the optimization of Slater determinant is proceeded what leads to the construction of the effective single-particle Hamiltonian \mathcal{H}^{eff} . Effectively, it reduces to fulfilling the condition that its optimal expectation value with $|\psi_0\rangle$ is coincident with that calculated diagrammatically for \mathcal{H} with $|\psi_G\rangle$,

$$\delta \langle \mathcal{H}^{\text{eff}} \rangle_0 (C_{1,l'}^{\alpha,\beta}, n_{0f}) = \delta \langle \mathcal{H} \rangle_G (C_{1,l'}^{\alpha,\beta}, n_{0f}) = \sum_{1,l',\alpha,\beta} \left(\frac{\partial \langle \mathcal{H} \rangle_G}{\partial C_{1,l'}^{\alpha,\beta}} \delta C_{1,l'}^{\alpha,\beta} + \frac{\partial \langle \mathcal{H} \rangle_G}{\partial n_{0f}} \delta n_{0f} \right), \quad (\text{S14})$$

where $\alpha, \beta \in \{f, c\}$. This yields following structure of \mathcal{H}^{eff} presented in the main text of the manuscript,

$$\begin{aligned}\mathcal{H}^{\text{eff}} &= \sum_{\mathbf{i},\mathbf{j}} t_{\mathbf{ij}} \hat{c}_{\mathbf{i}}^\dagger \hat{c}_{\mathbf{j}} + \sum_{\mathbf{i},\mathbf{j}} t_{\mathbf{ij}}^f \hat{f}_{\mathbf{i}}^\dagger \hat{f}_{\mathbf{j}} \\ &+ \sum_{\langle \mathbf{i},\mathbf{j} \rangle, \alpha=x,y} \left[iV_{\mathbf{ij}}^{\text{eff}} \left(\hat{c}_{\mathbf{i}}^\dagger \sigma_\alpha \hat{f}_{\mathbf{j}} + \hat{f}_{\mathbf{i}}^\dagger \sigma_\alpha \hat{c}_{\mathbf{j}} \right) + \text{H.c.} \right] + \sum_{\langle \mathbf{i},\mathbf{j} \rangle} \left(iV_{\mathbf{ij}}^{\text{eff}} \left[\hat{c}_{\mathbf{i}}^\dagger (\sigma_x - a\sigma_y) \hat{f}_{\mathbf{j}} + \hat{f}_{\mathbf{i}}^\dagger (\sigma_x - a\sigma_y) \hat{c}_{\mathbf{j}} \right] + \text{H.c.} \right) \\ &\equiv \sum_{\mathbf{k}} \hat{\Psi}_{\mathbf{k}}^\dagger \hat{\mathcal{H}}^{\text{eff}}(\mathbf{k}) \hat{\Psi}_{\mathbf{k}},\end{aligned}\quad (\text{S15})$$

The effective microscopic parameters determining \mathcal{H}^{eff} read (note that the c -electron hopping remains unchanged)

$$\begin{aligned}t_{\mathbf{ij}}^f \Big|_{\mathbf{i} \neq \mathbf{j}} &= \frac{\partial \langle \mathcal{H} \rangle_G}{\partial F_{\mathbf{i},\mathbf{j}}}, & V_{\langle \mathbf{i},\mathbf{j} \rangle}^{\text{eff}} &= \frac{\partial \langle \mathcal{H} \rangle_G}{i \partial W_{\langle \mathbf{i},\mathbf{j} \rangle_x}}, \\ t_{\mathbf{ii}}^f &= \frac{\partial \langle \mathcal{H} \rangle_G}{\partial n_{0f}}, & V_{\langle \langle \mathbf{i},\mathbf{j} \rangle \rangle}^{\text{eff}} &= \frac{\partial \langle \mathcal{H} \rangle_G}{(i-1) \partial W_{\langle \langle \mathbf{i},\mathbf{j} \rangle \rangle_{x=y}}}.\end{aligned}\quad (\text{S16})$$

General scheme

Finding equilibrium groundstate can be described in the following steps:

1. Diagrammatic evaluation of $\langle \mathcal{H} \rangle_G$ for the chosen $|\psi_0\rangle$.

2. Minimization of $\langle \mathcal{H} \rangle_G$ with respect to x .
3. Determination of the single-particle Hamiltonian \mathcal{H}^{eff} by optimization of $\langle \mathcal{H} \rangle_G$ with $|\psi_0\rangle$.
4. Determination the ground state, $|\psi'_0\rangle$ of \mathcal{H}^{eff} .
5. Repeating steps 1-4 in a self-consistent loop until a satisfactory convergence for $|\psi_0\rangle = |\psi'_0\rangle$ is reached.

CONVERGENCE WITH RESPECT TO THE ORDER OF EXPANSION

In Fig. S1 we present the resulting indirect gap value for $\varepsilon = -0.5$ (cf. Fig. 3(a) - main manuscript) for different orders of the diagrammatic expansion. We do not show results for $k = 0$ as on the recovered there mean-field level the topological Anderson lattice model with initially non-dispersive f -states is capable to describe only semi-metallic state with a zero gap. In the subsequent orders, $k > 0$ the nontrivial behavior of a gap can be seen. Starting from the second order, $k \geq 2$ the metallic state appears in the strongly correlated regime $U \gtrsim 10$. The practically overlapping values of the gap for $k = 4$ and $k = 5$ indicate that at this level of truncation of the order the satisfactory convergence is reached. Hence all results in the main manuscript are presented for $k = 4$.

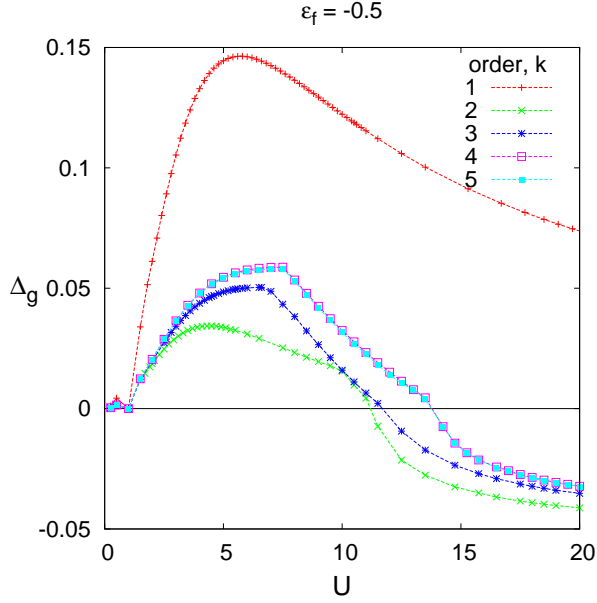


FIG. S1: Value of the indirect gap, Δ_g with respect to the interaction strength U . The negative value of the gap denotes the range of the mutual energy overlap between the upper and the lower hybridization bands in the metallic state. The points for $k = 4$ and $k = 5$ practically overlap indicating that satisfactory convergence with respect to order is reached.

* Electronic address: mwysoki@sissa.it

† Electronic address: fabrizio@sissa.it

- [1] J. Bünemann, T. Schickling, and F. Gebhard, *Eur. Phys. Lett.* **98**, 27006 (2012).
- [2] J. Kaczmarczyk, T. Schickling, and J. Bünemann, *Phys. Status Solidi b* **252**, 2059 (2015).